The onset of nonrigid dynamics and the melting transition in Ar7

François G. Amar and R. Stephen Berry

Citation: The Journal of Chemical Physics **85**, 5943 (1986); doi: 10.1063/1.451506
View online: http://dx.doi.org/10.1063/1.451506
View Table of Contents: http://scitation.aip.org/content/aip/journal/jcp/85/10?ver=pdfcov
Published by the AIP Publishing

The onset of nonrigid dynamics and the melting transition in Ar_7

François G. Amar
Department of Chemistry, University of Maine, Orono, Maine 04469

R. Stephen Berry
Department of Chemistry, University of Chicago and James Franck Institute, Chicago, Illinois 60637

(Received 16 June 1986; accepted 4 August 1986)

We have carried out a molecular dynamics (MD) simulation study of melting of Ar_7. By periodically quenching trajectories, we are also able to follow the path of the cluster through configuration space. This procedure yields information about isomerization rates, isomerization dynamics, and the connectivity of the phase space as a function of energy. New criteria for melting and the coexistence of phases in small clusters are compared with the traditional $T(E)$ curves and rms bond fluctuations available from time averages in MD simulations.

I. INTRODUCTION

This study is part of an overall attempt to understand the changes in physical behavior of a chemical system as its size is increased from the isolated molecule regime to a bulk phase. We have focused our attention here on the melting transition in very small clusters, bringing to this already much discussed subject,[1–10] a new perspective based on the ideas of the theory of nonrigid molecules,[10–13] and the concept of "hidden structure" in liquids introduced by Stillinger and Weber.[14–16]

A. Background

The literature on clusters and van der Waals molecules is very extensive and we cannot hope to summarize it completely here. The simulation work on rare gas clusters has its origins in attempts to calculate free energies of formation of these clusters as a function of size in order to determine critical cluster sizes for use in homogeneous nucleation theory. It was McGinty who noticed that the self-diffusion coefficient in the cluster rose dramatically at a fairly sharply defined internal energy for each cluster size.[1] Since then a great deal of work has been performed using both Monte Carlo (MC) and molecular dynamics (MD) techniques; these studies have reported "melting temperatures" (T_m) as a function of cluster size. Of particular interest is the relation between this transition and true phase transitions which can occur only in the thermodynamic (large N) limit.[17] One indicator of the cluster melting transition is the change in slope of E vs T from MC simulation.[4–7] The sharpness of this change in slope is a measure of how close to "macroscopic" the system is (in the limit of large N, this represents a discontinuous change in the heat capacity).

The paper of Hoare and Pal[18] also stimulated a great deal of work on the stable, low temperature structures of rare gas microcrystallites. This work has led to the theoretical prediction and the experimental observation of the so-called "magic numbers" for crystallites—clusters exceptionally stabilized by virtue of their filled concentric shells with characteristic icosahedral packing as opposed to the fcc packing expected for bulk systems. The electron diffraction work of the Farges group[19] and others[20,21] has clearly demonstrated the predominance of noncrystalline order for small clusters and the work of Northby's group among others has demonstrated that the charged rare gas clusters, at least, show the magic number phenomenon.[22]

B. Nonrigid molecules

Small clusters of atoms and molecules may be viewed as molecules in their own right, albeit with a large number of low frequency normal modes. van der Waals molecules are good candidates for demonstrating highly nonrigid behavior, because of their weak intramolecular interactions. The paper of Ezra[11] and the review of Natanson[12] provide surveys of some of the major contributions to the group theoretical treatments of nonrigid molecules and their interconnections. Common to these ideas is the notion of disparate time scales for large-amplitude "nonrigid" motions and small amplitude "rigid" motions.[10] The nonrigid molecule is thus described as executing oscillating motion about some local minimum in the potential hypersurface on a short time scale. These hops may occur via classical barrier crossing or by quantum mechanical tunneling. We shall be exclusively concerned with the former processes here.

C. Hidden structures

Stillinger and Weber have recently emphasized the utility of the nonrigid molecule conceptualization for describing liquid structures. In their hidden structure approach, they have shown that it is useful to view the body of liquid as a supermolecule with many (on the order of $\exp N$) local minima in its potential energy hypersurface. Rapid quenching of an arbitrary microscopic state of the system ($\mathbf{q}$ and $\mathbf{p}$ specified) drives the system to one of these local minima. In their method, the configurational part of the partition function of the liquid may be decomposed into a part which counts local minima and a vibrational contribution for each minimum.[14]

Stillinger and co-workers have applied quenching techniques to a number of systems including 2D model fluids,[14] liquid water,[15] and to the melting properties of simple fluids.[16] They have tracked the passage from potential well to potential well by keeping a record of the energy of successive quenches; these systems have been too large, however, to allow the possibility of following detailed dynamics of all the

 0021-9606/86/225943-12$02.10

particles for long times. We have undertaken a complementary study of a smaller system by coupling the quenching technique with MD simulations to study in a detailed way the path that a small cluster travels in configuration space. This approach leads to an improved understanding of the melting transition in small clusters and of the time scales required to establish ergodicity for particular phases.

While this paper is exclusively concerned with the Ar_7 cluster, a recent paper by Jellinek, Beck, and Berry[23] has applied some of these ideas to the Ar_{13} cluster though the quenching technique was not employed in that work.

II. METHODOLOGY

The Ar_7 cluster was chosen for this investigation because it is small enough to permit a detailed treatment in terms of collective coordinates (if required) and yet is large enough to display the melting features which are of general interest for small clusters. Briant and Burton (BB) have performed MD simulations[3] of argon clusters of various sizes in which they observed nonmonotonic behavior in plots of temperature vs energy. They call this portion of the $T(E)$ curve a "melting loop" and consider it to be evidence of a first-order-like phase transition in small clusters. The Ar_7 cluster was the smallest to display a loop in $T(E)$. In their MC calculations, Etters and Kaelberer (EK) use several criteria to determine melting temperatures.[5,6] The slope of V vs T changes abruptly in a narrow range of temperature (Ref. 5, Figs. 1 and 2). EK associate this temperature with melting. An apparently more reliable criterion for melting, especially for smaller clusters, is the temperature at which the magnitude of the root-mean-square bond length fluctuations abruptly doubles (Ref. 5, Fig. 5). While the MC and MD calculations employed identical potential parameters, different values of temperature were attributed to melting. Briant and Burton report that Ar_7 melts at about 20 K, i.e., the center of their $T(E)$ loop is at about 20 K, while Etters and Kaelberer's data indicates $T_m = 15.7 \pm 1.0$ K. Our MD results indicate that the onset of melting occurs at $T = 16.2 \pm 0.5$ K in agreement with the MC result. The melting loop observed by BB disappears when trajectories are run long enough to obtain good statistics.

We have chosen to perform molecular dynamics simulations of the Ar_7 cluster rather than Monte Carlo because we are interested in the real time dynamics of the melting transition, not just in phase space averages. For each energy of interest we select some initial phase points and integrate the classical equations of motion using an accurate integrator (fourth-order Adams–Moulton predictor–corrector, initialized by Runge–Kutta). A typical time step was 6.24×10^{-15} ps yielding energy conservation of about 1 part in 10^7 over as many as 9.6×10^6 steps (total of ~ 60 ns). The usual bin averages over energy and kinetic energy were performed, allowing the estimation of temperature and statistical uncertainty.

As in all straightforward MD calculations, a trajectory at a given energy yields equilibrium information using the standard averaging techniques.[24] The novel aspect of this study is the procedure used to halt the trajectory at regular intervals, and subject the system to a quenching procedure that seeks the local potential minimum. The standard IMSL-library routine, ZXMIN was used to quench the system and gave good results. By keeping a record of all the *different* minima found along the trajectory, it is possible to bracket the time of an isomerization event occurring between two successive quenches which find different minima in the potential hypersurface. For each energy we record the time steps at which isomerizations occur, the frequency of isomerizations, and E_{kin}, the time average of the kinetic energy. Additional information about the connectivity of the phase space (i.e., which isomers are accessible from other isomers) is obtained. The energy averages are performed for each isomer as well as for the whole trajectory.

Operationally, initial conditions are chosen by performing an MC simulation of the Ar_7 cluster at $T = 20$ K. This temperature is high enough to permit the system to sample energies near the dissociation limit. A large number of configurations are stored along with their energies and then we select configurations at equal energy intervals (about 3 K) but as widely spaced as possible along the Markov chain so as to reduce the configurational correlation of initial trajectories at adjacent energies. Then, by choosing the set of momenta $\{\mathbf{p}\}_0 = 0$, several simplifications of the problem are realized. First, the simplification of keeping the center of mass fixed is trivially obtained by conservation of linear momentum (this provides a check on the integration scheme). Second, and more important for our purposes, conservation of angular momentum dictates that the cluster is not initially rotating and will never rotate. The only "rotation" that will be observed is a "pseudorotation"[25] or isomerization. One caveat is in order: a degenerate vibration may give rise to an angular momentum which couples with overall rotation. It is then the sum of the two angular momenta which is conserved. We have not investigated the vibration–rotation coupling in this system; we have avoided explicit consideration of rotation–vibration interaction by choosing initial conditions for which $\mathbf{L} = 0$. Classically, the set of points with $\mathbf{L} = 0$ is a set of measure zero on the isoergic surface so we might expect some differences to arise from rotation–vibration interactions but we expect these differences to be small for the Ar_7 cluster. One can argue that as the cluster becomes large (i.e., macroscopic) overall rotation will have no effect on the internal degrees of freedom since the moment of inertia becomes so large.

The melting simulation consists of a series of molecular dynamics trajectories at different energies, each punctuated at regular intervals by quenches. The choice of the interval between quenches must be made carefully since if it is too short, computer time will be wasted. In addition, the average time interval between isomerizations depends on the energy since at low energy no isomerizations can occur ($E < E_2^0$) while at high energies the rate of isomerization may be high. The appropriate interval is determined empirically.

III. CHARACTERIZATION OF Ar_7

A. Geometric isomers

In order to follow the Ar_7 trajectories in a meaningful way, it is first necessary to establish some rules for identify-

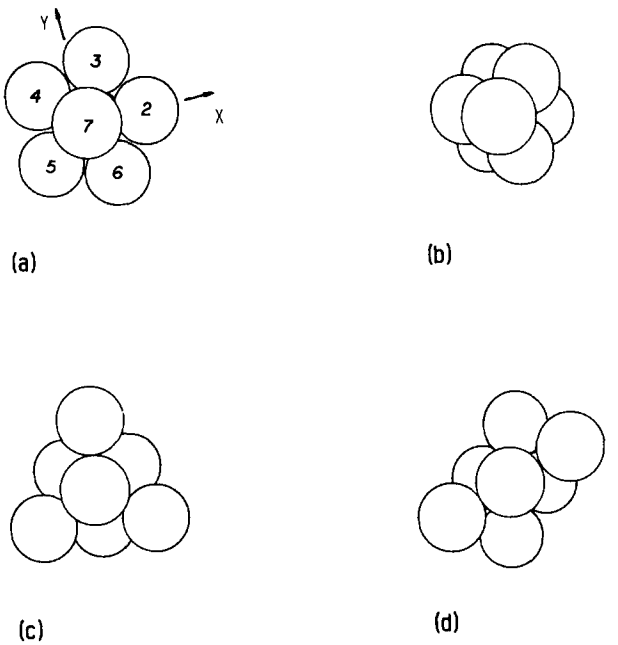

FIG. 1. The four local minima of Ar_7 (a) Pentagonal bipyramid $E_1^0 = -16.505\ \epsilon$. The numbering convention for PBP isomers is indicated. This isomer is denoted 205000:[7123456]. (b) Octahedron + 1, $E_2^0 = -15.935\ \epsilon$. (c) Incomplete stellated tetrahedron $E_3^0 = -15.593\ \epsilon$. (d) Skew structure $E_4^0 = -15.533\ \epsilon$. See the text for further discussion.

ing different isomers. The work of Hoare and Pal[18] indicates that a model of Ar_7 using Lennard-Jones 6-12 pairwise potentials has only four distinct geometric isomers. Our study confirms this: we find four and no more. We have used Lennard-Jones parameters: $\epsilon = 119.8$ K and $\sigma = 3.405$ Å for this calculation (the same as used by EK). The resulting geometric isomers are pictured in Fig. 1. Table I gives the energy of the equilibrium configuration for each geometric isomer as well as the number of nearest neighbor interactions and a code which permits specification of different isomers on the basis of numbers of atoms with 1, 2, 3, 4,... nearest neighbors. For example, the lowest energy isomer has the code 205000 which can be read from *right* to *left* as: no atoms with one, two, or three nearest neighbors, five atoms with four nearest neighbors, no atoms with five nearest neighbors, and two atoms with six nearest neighbors. The structure corresponding to this code is the pentagonal bipyramid (PBP). Note that while structures 2, 3, and 4 all have 15 nearest neighbors, they have different nearest neighbor codes. The nearest neighbor code *appears* to be redundant in identifying the geometric isomer. Its use facilitates the description of the geometry of a cluster and also allows for the identification of previously unidentified isomers that might appear in the simulation of Ar_7 or larger clusters. There is the possibility for larger clusters that two isomers could have the same nearest neighbor code and different geometries. In such a case, energy would still distinguish the isomers, as it does for the bulk simulations of Stillinger *et al.*[14–16]

TABLE I. The minimum energy of the four Ar_7 geometric isomers is given in column 2. Columns 3 and 4 are the number of nearest neighbor interactions and the nearest neighbor code, respectively. The MS group designation, the order of the MS group, and the number of distinct permutational isomers are also given for each geometric isomer.

Isomer	Energy (ϵ)	N–N	N–N code	MS group	Order	n_i^*
1 (PBP)	−16.505	16	205 000	D_{5h}(M)	20	504
2 (OCT + 1)	−15.935	15	33 100	C_{3v}(M)	6	1080
3 (IST)	−15.593	15	130 300	c_{3v}(M)	6	1080
4 (SKEW)	−15.533	15	122 200	C_2 (M)	2	5040

B. Permutational isomers

Since this study involves the use of classical mechanics, we must also account for permutational isomers of the same geometry and apply a correction factor (symmetry number) to compare to quantum mechanics. Thus we need to distinguish not only between geometric isomers but also between different permutational isomers of the same geometry. Our treatment follows the notation of Bunker.[13]

The complete nuclear permutation inversion (CNPI) group for a molecule with seven identical atoms is the direct product of the permutation group of order seven and the inversion group: CNPI $= S_7 \otimes \{E, E^*\}$. This group contains $(2\times 7!) = 2\times 5040 = 10\,080$ elements. For each distinct geometric isomer, we need to know the number of elements of the CNPI group which return a given labeled structure to itself; i.e., we need to determine the molecular symmetry [MS] group. Then, the number of distinct permutational isomers is the order of the CNPI group divided by the order of the MS group.

Let us examine the pentagonal bipyramid in some detail and simply state the results for the other rigid structures. The MS group for the PBP contains 20 elements, is isomorphic to the point group D_{5h}, and is given the label $D_{5h}(M)$ to distinguish it from the point group itself. The distinction between the MS group $D_{5h}(M)$ and the point group D_{5h} is that the former is a symmetry group of the molecular Hamiltonian while the latter is a near symmetry group of the molecular Hamiltonian and a true symmetry group of the vibronic Hamiltonian.[13] Figure 1 illustrates the labeling convention that we use. If particles 7 and 1 are the axial argon atoms in the PBP we place the molecule fixed z axis along the vector from 1 to 7 (i.e., the higher numbered atom in the positive direction). Then the molecule fixed x axis (right-handed coordinate system) is oriented towards the equatorial atom with the smallest number and the remaining atoms are counted off counterclockwise (in the positive ϕ direction). Thus the permutational isomer of the PBP shown in Fig. 1 is specified by the code 205000:[7123456]. The elements of $D_{5h}(M)$ consist of those permutations or permutation/inversions which exchange nuclei to a configuration that can be brought back to the original by a simple rotation. These are called "feasible" permutations. So (17) and E^* are not elements of $D_{5h}(M)$ for the isomer of Fig. 1(a) but the product operation $(17)^*$ is. The number of distinct permutational isomers of PBP geometry (each having a separate MS group) is, according to our formula, $10\,080/20 = 504$. The additional columns in Table I list the MS group designations, the order of the groups, and the

number of distinct permutational isomers for the other geometric isomers of Ar_7.

The isomer names given in Fig. 1 are the same as those employed by Hoare and Pal (HP).[18] Our isomer energies are identical to five places with those of HP (ours are slightly lower) and, judging by their figures and discussion, the structures are the same as well. It appears, however, that HP assign symmetry groups incorrectly to the geometric forms of three of the isomers of Ar_7. They assign the octahedron + 1 (OCT + 1) isomer to the C_2 point group when it actually has C_{3v} symmetry. Similarly, the incomplete stellated tetrahedron (IST) is C_{3v} not D_3 and the skew structure (SKEW) of isomer 4 has C_2 not C_1 symmetry.

HP make a few other errors of this sort: notably, the assignment of the equilateral trimer to C_3 rather than D_{3h} and the assignment of the Ar_6 tripyramid to C_{2h} rather than C_{2v}; while these errors invalidate the use of point groups as a descriptive device, they appear to be fairly inconsequential as far as rest of HP's discussion is concerned. We must emphasize, however, that for *our* work it is essential to assign the symmetry groups of the isomers of a small cluster correctly. Incorrect symmetry assignments can lead to errors in symmetry numbers, numbers of permutational isomers, and density-of-state functions.

IV. TRAJECTORY RESULTS

The trajectories we have analyzed fall quite naturally into three groups characterized by energy relative to the barriers to isomerization. The barriers (or, rather, the lowest energy saddles) between different isomers have not been determined. However, the barrier between any two isomers must have an energy higher than the higher of the two potential energy minima associated with the two isomers. It is also clear from the principle of equipartition of energy that the total internal energy of the cluster must be somewhat higher than the barrier itself in order for enough energy to accumulate in the reaction coordinate to take the system from one isomer to another on the time scale of the simulation.

TABLE II. Summary of MD trajectories for Ar_7. From left to right the columns list: a number code proportional to energy; the energy (in units of ϵ); the temperature T (in K) computed from the time averaged kinetic energy; 95% confidence limits on T; the total isomerization rate (1/ns).

Trajectory No.	Energy	T	ΔT	*iso*/ns
010	−16.0780	3.36	0.003	...
030	−15.5787	7.15	0.008	...
050	−15.0731	10.80	0.01	...
075	−14.4494	14.98	0.15	0.20
079	−14.3391	15.62	0.17	0.40
080	−14.3141	15.87	0.10	...
081	−14.2898	15.83	0.26	1.00
082	−14.2681	16.12	0.10	...
083	−14.2434	16.23	0.17	1.21
084	−14.2162	16.39	0.08	1.05
085	−14.1879	16.10	0.23	2.39
086	−14.1739	16.38	0.18	2.01
087	−14.1436	16.56	0.28	2.28
088	−14.1164	16.81	0.09	2.54
089	−14.0962	16.92	0.28	2.08
090	−14.0644	16.98	0.17	2.83
091	−14.0390	17.17	0.21	2.88
092	−14.0202	17.22	0.24	4.48
095	−13.9468	17.71	0.29	4.34
100	−13.8203	18.28	0.21	8.36
110	−13.5611	19.37	0.33	19.94
115	−13.4352	19.63	0.21	26.56
120	−13.3180	20.39	0.25	32.18
125	−13.1803	20.79	0.16	30.7
130	−13.0635	21.22	0.55	63.7
187	−11.6300	27.99	0.19	522

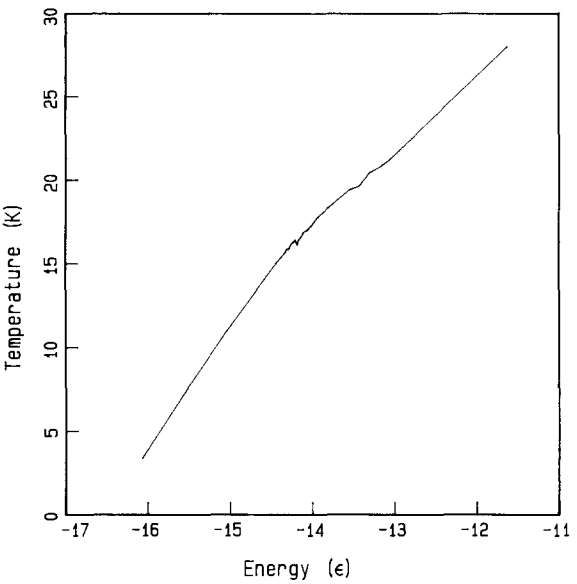

FIG. 2. T vs E for Ar_7. Our results show no melting loop of the magnitude and at the position found by BB (see Ref. 5, Fig. 1). The melting region between $T = 16$ and 20 K is characterized by large fluctuations in T.

The three groups of trajectories are identified with the solid form of the cluster (low energy), the liquid form (high energy), and an intermediate form which may be identified with the "melting region" or better, the "coexistence range" described previously.[10,26] Table II summarizes the general results of a number of trajectories. Figure 2 shows the T vs E curve (caloric equation of state) with the two monotonic branches at low and high energies and the melting region at intermediate energy. We shall refer to these results in the discussion below.

A. Solid clusters

Empirically, the low energy trajectories are those for which no isomerizations are observed even after very long times. At low energies, the clusters are trapped in one of the isomeric geometries (usually the lowest) whose potential minimum lies below the cluster energy. The trajectories are relatively uneventful but nevertheless are useful in that we can obtain excellent statistics for the T vs E curve in MD simulations in order to establish a base line for the intermediate portion of this curve. We obtain T from the kinetic energy average $E_{\rm kin}$ defined by

$$E_{\rm kin} = \frac{1}{n_t} \sum_{j=1}^{n_t} \sum_{i=1}^{N} \frac{\mathbf{p}_i^2}{2m_i}, \tag{1}$$

where n_t is the total number of time steps, and then

$$T = \frac{2E_{\text{kin}}}{3N-6}. \tag{2}$$

In our case $N = 7$. We exclude center-of-mass motion and overall rotation from our count since our initial conditions prohibit any contribution to the kinetic energy from these degrees of freedom.

B. Liquid-like clusters

In contrast to the low energy trajectories, the high energy trajectories are characterized by a high rate of isomerization. At high energy, the system samples all the available phase space and displays the characteristics of a liquid. The different isomeric regions that the system visits each contribute a distinctly different range of values of E_{kin} to the overall time average; however, the rate of isomerization is sufficiently high at high energy that for long runs this variation is averaged out and the caloric (T vs E) curve is monotonic once more. One indicator of this is that the standard deviation of T shown in Table II is much smaller than that for the intermediate region. We will return to a discussion of the high energy trajectories when we consider residence times.

C. The melting region

The lowest energy for which we observe isomerizations is $E = -14.45\,\epsilon$. This energy is still so low, however, that very long trajectories (1500 ps) are required to observe just one or a few isomerizations. The total energy of the system is clearly high enough for the system to exist in any of the four geometric isomers. Nevertheless, not all isomers are observed. We do not know whether this is due to the presence of a saddle above $-14.45\,\epsilon$ which absolutely prevents passage or whether the rate of isomerization is so slow across a high saddle that it cannot be observed in runs of reasonable length.

We see no evidence for the melting loop at 20 K that was observed by BB; our results are consistent with recent results for Ar_{13}.[23] We do observe in the region between $E = -14.25\,\epsilon$ and $E = -13.3180\,\epsilon$ (corresponding to temperatures between 15 and 20 K), that the rate of isomerization is very low and the corresponding lifetimes (especially of the PBP) are very long. In this region we observe a *small* number of what Schiferl and Wallace call "level shifts."[27] At a given total energy, each isomer has a characteristic E_{kin} and therefore its own "temperature." In relatively short runs, reliable estimates of the temperature of each isomer can be made but no reliable estimate of the overall temperature is feasible since the system may become trapped in one isomeric form for a disproportionate amount of time.

The only way around this problem is to make longer runs. Most of our trajectories were of 15 ns duration. In the melting region we extended some of these runs to 30 ns and for 2 points we ran trajectories for 45 and 60 ns (9.6×10^6 time steps). Figure 3 shows the well-averaged T vs E curve in the melting region together with 95% confidence limits on

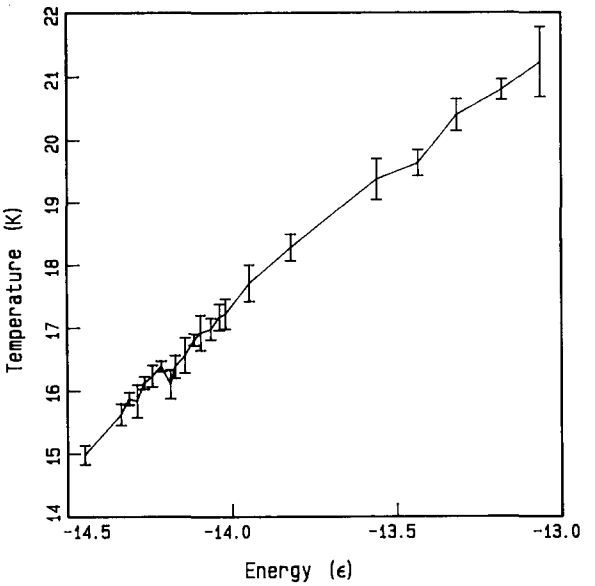

FIG. 3. T vs E for Ar_7. The melting region is shown with 95% confidence limits for T [see Eqs. (3) and (4)]. For runs of uniform length, the uncertainty limits are largest in the melting region. We have run longer trajectories in this region in order to reduce the error bars in the coexistence region.

T. The 95% confidence limit is given by

$$\langle T \rangle = \overline{T} \pm \alpha_n \frac{s}{n^{1/2}}, \tag{3}$$

where

$$s = \left\{ \frac{1}{n-1} \sum_{k=1}^{n} (T_k - \overline{T})^2 \right\}^{1/2}. \tag{4}$$

Here α_n is the 0.975 fractile of Student's t distribution for n observations.[27] We varied n by averaging over fewer (more) bins of greater (shorter) length and report here the minimum uncertainties from the sets of confidence limits so obtained. Even with our long runs our uncertainty in T remains in the neighborhood of 0.1 to 0.2 K at best.

Even with these uncertainties in $T(E)$, the data do preclude a melting loop of the magnitude and at the position found by BB. A look at Table I shows why BB found the loop that they did. Their runs were no longer than 0.1 ns and our isomer lifetime data show that the average lifetime of the PBP is significantly longer than 0.1 ns until the temperature reaches about 20 K. Thus their trajectories were trapped in the well of the most probable isomer until the cluster was sufficiently hot that the lifetime of the PBP isomer became comparable to or shorter than the length of the run. For a cluster at $E = -13.318\,\epsilon$, the long run average $T = 20.4$ K. The E_{kin} value for PBP isomers separately yields a value of $T = 21.65$ K. The residence-time weighted average of E_{kin} for isomers 2, 3, and 4 yields a value of $T = 17.22$ K. The difference between these last two temperatures, $\Delta T = 4.42$ K, is an upper limit for the crest to trough height of an Ar_7 melting loop at $T \cong 20$ K. The crest to trough height of BB's melting loop for Ar_7 is estimated (from Ref. 3, Fig. 1) to be $\Delta T = 4.3$ K. Our upper limit to the loop height is based on three assumptions: (1) Only the lowest isomer contributes to the kinetic energy average for the crest. (2) Only isomers 2, 3, and 4 contribute to E_{kin} for the trough. (3) The trajec-

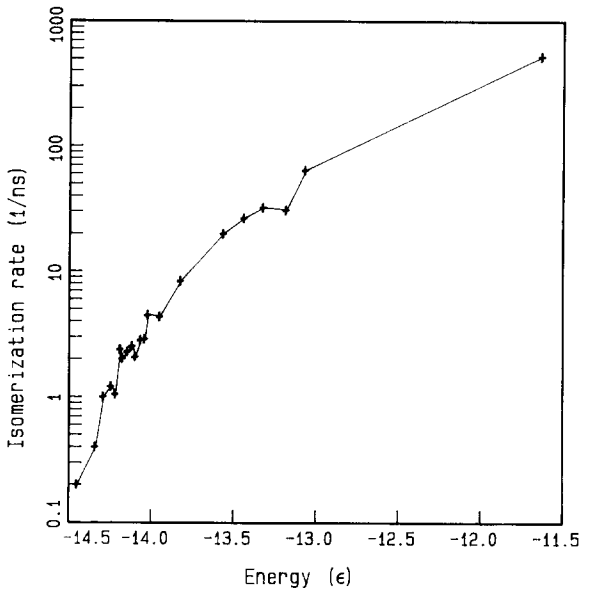

FIG. 4. Isomerization rate vs energy. Up to $E = -14.039\,\epsilon$, we have used a quench interval of ~ 6.28 ps. Beyond that energy our quench interval is ~ 2.49 ps. At the highest energy studied, we quenched every 0.15 ps. At the high energy there is a tendency to underestimate the rate since some isomers survive for less time than a quench interval. On the other hand, rapid recrossing may lead to an overestimate of the rate.

tory is long enough that E_{kin} for each isomer is reliably determined. Our lifetime data indicate that the first assumption is valid or nearly so. Likewise assumption (3) appears to be reasonable given our trajectory data. The second assumption is the most questionable especially since we have limited information about BB's trajectories. Our quenching data indicates that there *are* portions of a trajectory at $E = -13.318\,\epsilon$ ($T \cong 20.4$ K) in which the cluster shuttles back and forth between isomers 2, 3, and 4 without visiting isomer 1 for times equal to or greater than 0.1 ns.

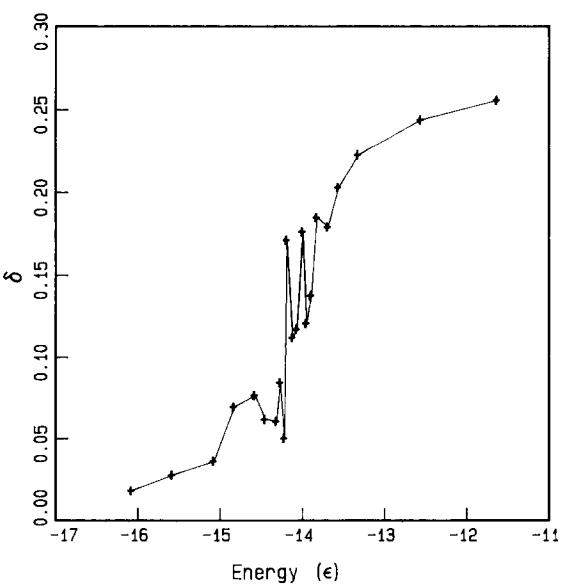

FIG. 5. Average bond length fluctuation δ vs E [see Eq. (5)]. Note the large fluctuations in δ in the melting region. δ jumps abruptly from about 0.1 to 0.2 at $E = -14.2\,\epsilon$ ($T = 16.2$ K).

Returning once again to Fig. 3, we see that there may be a nonmonotonic portion of the curve (a "microloop") at $E = -14.2162\,\epsilon$ ($T \cong 16.2$ K). We have run trajectories corresponding to the crest and trough of the microloop for 45 and 60 ns, respectively. Our 95% confidence limits indicate that we cannot be at all sure that the loop is real. This data really serves to underscore the fact that, in the coexistence region, we *must* look at very long trajectories in order not be misled by long dwell times.

In Fig. 4 we plot the rate of isomerization vs energy. There are, once again, significant fluctuations in this curve due to statistical uncertainty. There is, however, a doubling in the rate of isomerization between $E = -14.2162\,\epsilon$ and $E = -14.1879\,\epsilon$ which is just the position of the microloop. This shift appears to be more than just a local fluctuation, since the rate never again decreases below 1.0 ns^{-1}. The temperature at which this shift in rate occurs is between 16.10 ± 0.21 and 16.3 ± 0.08 K. This temperature is consistent, within our respective uncertainty limits with the EK result ($T_m = 15.7 \pm 1.0$ K) and with other indicators of melting described below.

We have calculated for some of our trajectories, the rms fluctuation in the Ar–Ar bond lengths:

$$\delta = \frac{2}{N(N-1)} \sum_{i<j} \frac{(\langle r_{ij}^2 \rangle_t - \langle r_{ij} \rangle_t^2)^{1/2}}{\langle r_{ij} \rangle_t} . \tag{5}$$

This quantity was calculated for trajectories of uniform length (time = 1.5 ns). In Fig. 5 we plot δ vs energy. The value of δ increases dramatically through the melting region in accord with previous MC and MD results.[3,5] As expected, the uncertainty in δ is very large in the melting region as evidenced by large oscillations in value for neighboring energies. These averages were carried out for runs of 1/10 the length of the typical T vs E runs.

Whether or not the details of the microloop and the rate shift are correct it is clear that the onset of isomerization occurs at about $E = -14.1\,\epsilon$, $T \cong 16.0$ K. The increase in δ compares well with the corresponding quantity in the MC calculation of EK. That is, δ exceeds 10% at $E = -14.1\,\epsilon$ or $T = 16.2$ K in accord with the Lindemann criterion.[5]

V. DYNAMICS

MD simulation of Ar_7 coupled with the quenching technique provides dynamical information about the system because the configuration of the cluster can be tracked as a cluster samples the available phase space. This dynamical information can be extracted in various ways from the trajectories.

At the most elementary level we can simply compute the time that Ar_7 spends as each type of geometric isomer, summing over the whole trajectory. These *residence times*, discussed below, are a measure of the equilibrium between isomers to the extent that our time averages properly reflect microcanonical ensemble averages. At the next level of complexity, we look at the distribution of isomer lifetimes τ as a function of energy. The *lifetime distributions* change markedly through the coexistence range and into the liquid region.

Finally we present isomerization rate information in the

TABLE III. MD and statistical residence times for three trajectories representative of the solid, melting region, and liquid, respectively.

$E=-14.4494$ $T=14.98$		$E=-14.1879$ $T=16.10$		$E=-13.0635$ $T=21.22$	
MD	Stat	MD	Stat	MD	Stat
0.981	0.964	0.867	0.933	0.596	0.712
0.019	0.0341	0.100	0.0597	0.211	0.188
0.0	0.0009	0.0128	0.0028	0.0623	0.0319
0.0	0.0012	0.0195	0.0046	0.131	0.0682

form of *frequency tables* and *rate tables*. These tables indicate how often an isomer of geometry j is obtained from an isomer of geometry i, and provide a measure of the connectivity of the phase space at each energy.

A. Residence times

The molecular dynamics program, as it has been implemented here, provides us with accurate information about the time that the system spends in regions of phase space which map via quenching to different geometric isomers of Ar_7. Table III shows the fraction of time spent in each of the four geometries for three different trajectories, representative of the low, intermediate, and high energy regimes. At low energy, only the lowest isomer is observed. At intermediate energy, the system spends most of its time as the most stable isomer. At high energies there is an oscillation in the residence times. Most striking is the fact that the isomer with the highest energy is much more probable than the one below it although the energies of these two are actually quite close.

The question arises: is this inversion of residence times due to specific dynamical effects of barriers or can it be explained in a statistical way? In fact the answer is that a statistical argument does explain the inversion.

We construct the simplest possible statistical model of the cluster density of states in order to investigate the residence times. Clearly the residence time in any region of phase space should be proportional to the density of states in that region. Since we are considering clusters which do not rotate or translate, it suffices to model the vibrations of the cluster to calculate the density of states.

In modeling the vibrations of the cluster, we make every possible simplifying approximation in order not to have to face the difficult task of calculating the exact density of states of sets of highly anharmonic oscillators. Each isomer is treated as a 15-dimensional isotropic harmonic oscillator and furthermore, we assign the same force constant to each isomer. The classical expression for the density of states of an isotropic oscillator is easily obtained[28]:

$$\omega(E-E_i^0)=\left(\frac{E-E_i^0}{h\nu}\right)^{m-1}\frac{1}{2^m(m-1)!h\nu}, \qquad (6)$$

where E_i^0 is the minimum energy of the ith geometric isomer. Since all the oscillators have the same force constant, the only difference in the density of states of the various isomers arises from the fact that each has a different minimum energy. The relative residence times in two different isomers is then given by $(E-E_j^0)^{m-1}/(E-E_i^0)^{m-1}$. One further correction must be applied. In order to avoid overcounting the phase space by counting regions which differ only by a rigid body rotation we should divide $\omega(E-E_i^0)$ by the appropriate symmetry number. The same effect is achieved by multiplying each density $\omega(E-E_i^0)$ by the number of distinct permutational isomers, n_i^*. This is easy to see since the number of distinct permutational isomers of a given geometry is equal to the order of the complete nuclear permutation (CNP) group S_7 divided by the order of the proper subgroup of the MS group (the symmetry number). The fractional residence time in all isomers of type i is then given by

$$t_i=\frac{n_i^*(E-E_i^0)^{m-1}}{\Sigma_j n_j^*(E-E_j^0)^{m-1}}. \qquad (7)$$

The results are listed in the second column of Table III. For low energies there is substantial agreement, with the lowest isomer dominating. Of course the statistical model can never give zero residence time for an energetically accessible isomer. For high energies there is good agreement indicating that the residence times are statistical at high energies. This

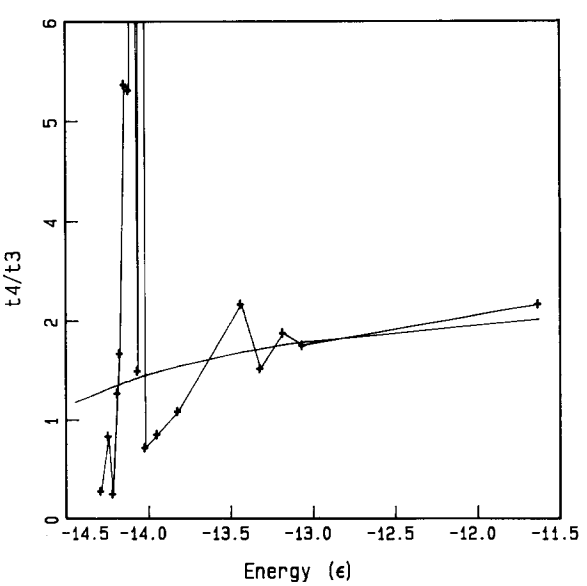

FIG. 6. Ratio of residence time in isomer 4 to isomer 3. The ratio t_4/t_3 tends to 3 in the statistical limit. The crosses (+) are the MD results while the smooth curve is the statistical result [Eqs. (6) and (7)]. The large change from negative to positive deviation from the statistical limit occurs at the onset of melting.

is not so surprising since if the energy of the system is much higher than the barriers or saddles in the hypersurface, they should act as small perturbations to the passage through phase space. The real disagreement between statistical theory and the simulation occurs in the coexistence region.

This nonstatistical behavior is most strikingly demonstrated in Fig. 6, in which we plot the ratio of residence time in isomer 4 to that in isomer 3. For comparison, we also plot the expected statistical ratio. This ratio is expected to be quite sensitive to barrier effects since the energies of the well minima are so close. At low energy the observed (MD) ratio is smaller than the statistical result. In the intermediate region, there is a dramatic spike in this ratio indicating a strong barrier effect. At higher energies the ratio of residence times agrees with the statistical prediction as both approach the high energy limiting value $t_4/t_3 = 3$.

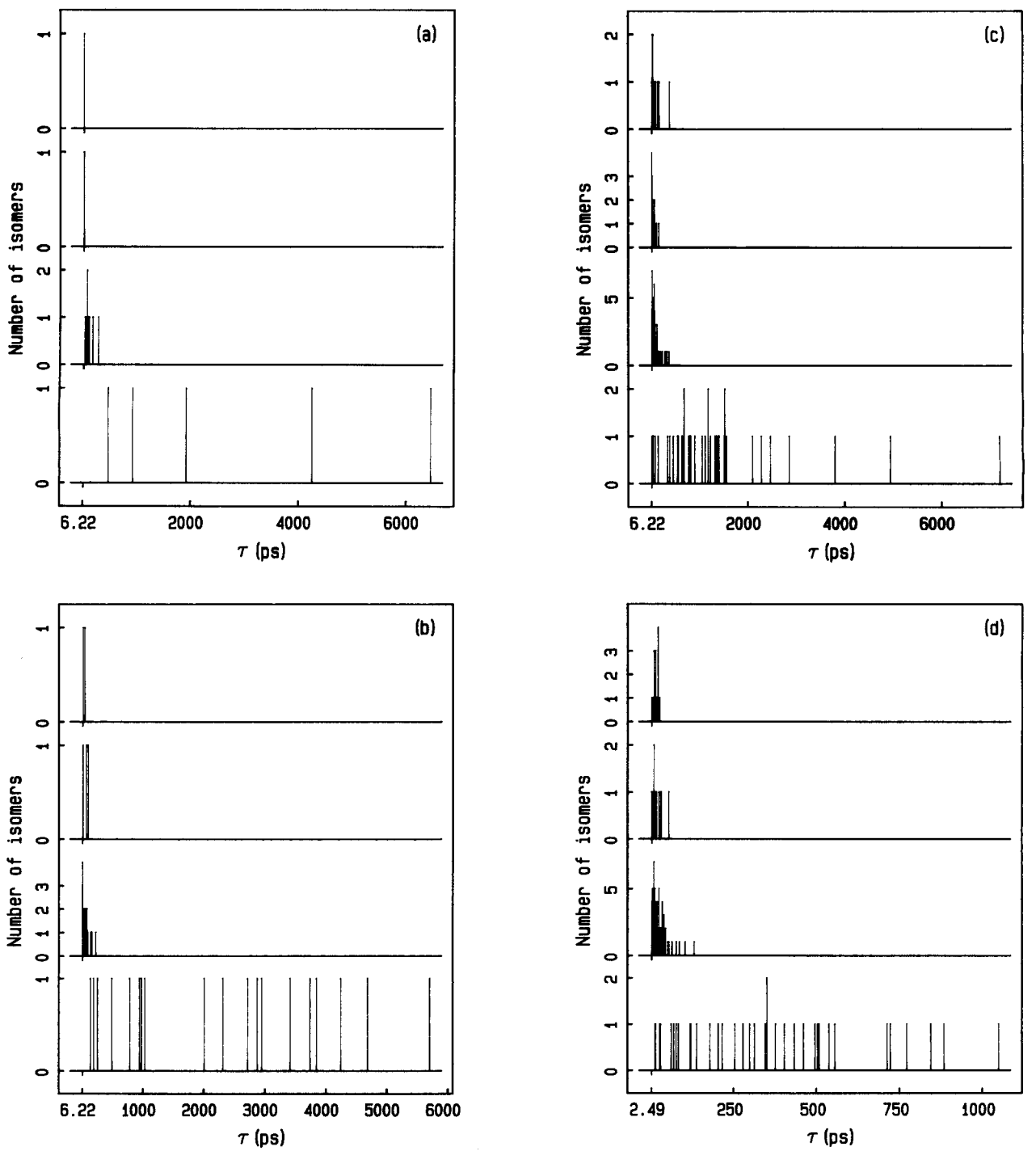

FIG. 7. Isomer lifetime distributions. In each panel the distributions are given for each of the four isomer geometries with lowest energy isomer (PBP) at the bottom and the highest energy geometry at the top. Each panel corresponds to a different energy trajectory as follows: (a) $E = -14.2898\,\epsilon$, $T = 15.83$ K (solid); (b) $E = -14.2162\,\epsilon$, $T = 16.39$ K (coexistence); (c) $E = 14.1879\,\epsilon$, $T = 16.10$ K (coexistence); (d) $E = -13.8203\,\epsilon$, $T = 18.28$ K (coexistence); (e) $E = -13.0635\,\epsilon$, $T = 21.22$ K (liquid); (f) $E = -11.6300\,\epsilon$, $T = 27.99$ K (liquid). See the text for discussion.

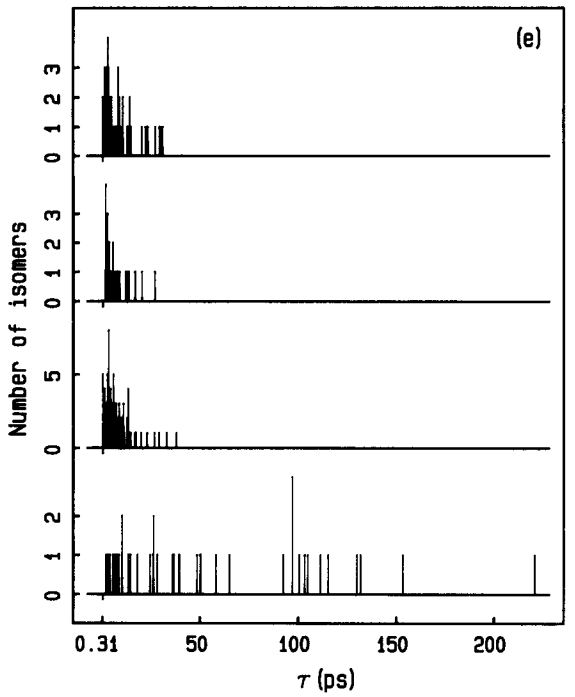

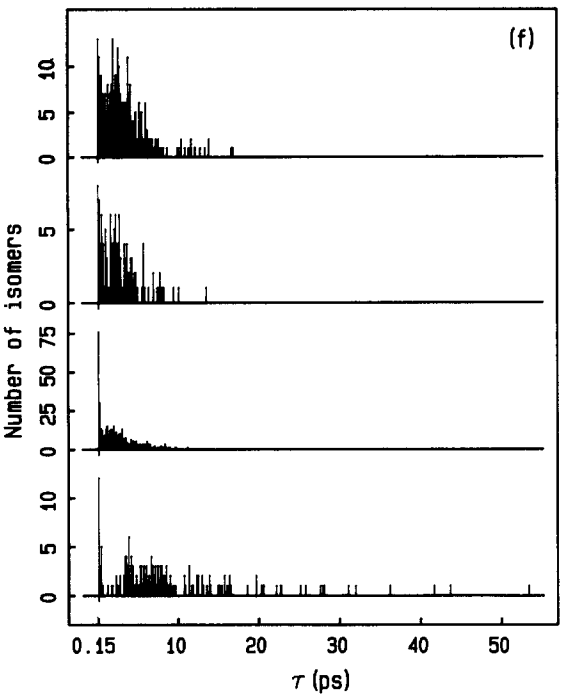

FIG. 7. (*continued.*)

McGinty has noted that the harmonic oscillator partition functions yield more accurate free energies than expected for clusters.[1] This is because of cancellation of errors of opposite sign: The harmonic oscillator density of states is too low because the variation of energy level spacing is constant, and it is too large because there is no dissociation limit.

B. Lifetime distributions

In Figs. 7(a)–7(f) we present a series of stick plots or histograms which represent the distribution of isomer lifetimes over a range of energies from below the coexistence region to well into the "liquid" regime. The height of each stick is proportional to the number of occurrences of a given geometric isomer with a lifetime between τ and $\tau + \Delta\tau$ ps. Here $\Delta\tau$ is the quench interval for the trajectory and is given below the first τ-tic label on the plot. As shown in Fig. 7(f), for example, at the highest energy studied, 13 PBP isomers lived less than one quench interval or between 0 and 0.15 ps.

From low [Fig. 7(a)] to high [Fig. 7(f)] energy, the scale of lifetimes shifts dramatically to shorter times. At the lowest energy shown, below the "onset" of melting but still above the point where isomerizations cease completely, the longest lived isomer lasts for about 6500 ps. At the highest energy shown, which corresponds to a liquid, 50 ps is the maximum lifetime.

In addition, as one looks to higher energies, the *range* of lifetimes of the PBP isomers becomes comparable to the range of lifetimes for the other isomers. These observations are consistent with our picture of the cluster as a nonrigid molecule whose fluxional character increases with total energy.

Several more subtle effects can also be noted in Fig. 7. At low energy [Fig. 7(a)], the set of lifetimes for the PBP does not overlap with the set of lifetimes for the other Ar_7 isomers. This situation is approximately preserved at the next energy shown, $E = -14.2162$ [Fig. 7(b)] which corresponds to the top of the microloop discussed in Sec. IV. In Fig. 7(c), which corresponds to the trough of the microloop, there is a substantial number of PBP isomers which live for very short times. The overlap of the short lived tail of the PBP lifetime distribution with the distributions of the other isomers becomes more pronounced in the liquid region [Figs. 7(e) and 7(f)]. We interpret the overlap behavior in the following way: In the solid region, the system remains trapped for a long time in a particular PBP isomer and may occasionally undergo isomerization. In the liquid regime, on the other hand, the cluster makes frequent hops from one isomer to another, visiting all regions of the accessible phase space. In the intermediate region we see some long lived PBP isomers which correspond to the "solid" and some short lived PBP isomers which contribute to the liquid phase properties. This behavior is evidence for the coexistence phenomenon previously postulated by us.[10,26] Strongly analogous behavior is observed in Ar_{13}, except in that case, bimodal kinetic energy distributions in the coexistence region serve the diagnostic role of our lifetime distribution plots.[23]

Let us focus, finally, on the very short lifetime portion of the lifetime distributions of the liquid clusters [Figs. 7(e) and 7(f)]. The quench interval is chosen to be very short for these trajectories in order to capture the fast isomerizations. Figure 7(f) shows maxima in the first lifetime bin, a subsequent decrease in number of isomers with slightly larger lifetimes, and finally there is a second rather broad maximum in the lifetime distributions at around 3 ps. This observation has interesting implications for our calculation of isomerization rates. We shall discuss this at greater length in the next section.

C. Frequency tables

The MD technique, coupled with the quenching algorithm, also provides information about the occurrence of isomerizations from an isomer of one geometry to isomers of different geometry (or different permutational isomers of the same geometry). This information is collected in a set of frequency tables for different energies. As shown in Table IV, each entry gives the number of times an isomer of type j (columns) was reached from an isomer of type i (rows). Note the high degree of symmetry in the matrix, resulting in part from the sum rules: $\Sigma_i f_{ij} = \Sigma_i f_{ji}$. If we divide f_{ij} by the time t_i that the system spends in isomers of type i we obtain a rate table as in Table V. The entries in Table V are essentially unimolecular rate constants k_{ij} for the isomerization reactions $i \rightarrow j$. At the lowest energy shown, only isomers 1 and 2 are observed. Through the melting region up to $E = -13.5611\ \epsilon$ ($T \cong 19.4$ K) the frequency tables have nonzero entries only in the second row and second column. Isomer 2 acts as an intermediate between all the other isomers in the coexistence region.

If we assume that the isomerization rates are governed by the barrier heights (lowest-energy saddle-point energies) between isomers, the k_{ij} tables permit us to roughly order activation barriers for isomerization, E^*_{ij}:

$$E^*_{12} < E^*_{23},\ E^*_{24} < E^*_{33} < E^*_{13},\ E^*_{14},\ E^*_{34} < E^*_{11},\ E^*_{22} < E^*_{44}. \quad (8)$$

It is possible to get estimates of these ten quantities by treating them as parameters to be fit in a transition state theory calculation[28] of the rates k_{ij} using (for example) harmonic oscillator density-of-states models. This would clearly be a very crude estimate of the barriers inasmuch as we do not really know anything about the transition state or even whether the isomerization coordinates are unique. Moreover, there are more accurate and convenient methods available for obtaining the barrier heights: As pointed out by LaViolette and Stillinger,[16] the Hessian matrix for the system will have negative eigenvalues at the saddle points. The corresponding eigenvector is the isomerization reaction coordinate. The details of the saddle point energies and the reaction coordinates will be addressed in a future communication.

A final point concerning the f_{ij} data presented in Table IV: At high energies one could argue that we have seriously *underestimated* the isomerization rates because our quenching interval is too large. At the highest energy studied ($E = -11.63\ \epsilon$, $T \cong 27$ K) our quenching interval was 0.156 ps. On the order of 10% of the observed isomers have lifetimes less than or equal to this interval. The situation is further complicated by the fact that rapid recrossing of the barrier is frequently observed at high energies. Berne and coworkers have shown[29] that isomerizations followed by rapid recrossing do not contribute to the reactive flux. Thus we may, in fact, be *overestimating* the isomerization rates in the high energy regime. The short lifetime behavior shown in Fig. 7(f) illustrates this problem in a very clear way.

At present it is not clear how rapid a rapid recrossing is in the Ar_7 system. We are, after all, dealing with a nonlinear dynamical system of 15 degrees of freedom. A hint as to the time scale to use to assess the effects of rapid recrossing is given by the occurrence of the relative minimum in the number of isomers at short time in Fig. 7(f). We shall explore the question of isomerization kinetics further in another paper.

TABLE IV. Frequency tables for a series of energies. The trajectories were run for 15 ns except for $E = -14.216$ which was run for 45 ns, $E = -14.188\ \epsilon$ which was run for 60 ns, and $E = -11.630\ \epsilon$ which was run for ~ 3.7 ns. The entries in each matrix give the (raw) number of isomerizations from an isomer of type i (rows) to one of type j (columns).

$E = -14.449$		$T = 14.98$		$E = -13.820$		$T = 18.28$	
0	1	0	0	0	35	0	0
2	0	0	0	36	2	9	16
0	0	0	0	0	10	0	0
0	0	0	0	0	15	1	1
$E = -14.290$		$T = 15.83$		$E = -13.561$		$T = 19.37$	
0	4	0	0	0	59	1	9
5	0	2	1	62	2	31	43
0	2	0	0	1	34	0	1
0	1	0	0	6	43	4	2
$E = -14.216$		$T = 16.39$		$E = -13.435$		$T = 19.63$	
0	17	0	0	5	155	10	15
17	1	4	2	151	37	63	121
0	4	0	0	13	61	0	8
0	2	0	0	16	119	9	10
$E = -14.188$		$T = 16.10$		$E = -13.318$		$T = 20.39$	
0	36	0	0	1	90	5	15
36	4	19	15	94	12	43	73
1	18	0	0	8	44	0	2
0	15	0	0	8	76	6	4
$E = -14.039$		$T = 17.17$		$E = -13.063$		$T = 21.22$	
1	16	0	1	0	31	2	7
17	1	0	3	32	0	27	49
0	0	0	0	2	29	0	1
0	4	0	0	7	47	3	1
$E = -13.947$		$T = 17.71$		$E = -11.630$		$T = 27.79$	
0	19	2	0	0	102	17	45
22	0	4	6	103	23	94	179
0	6	0	0	17	97	6	7
0	6	0	0	44	176	11	55

VI. CONCLUSIONS

We have presented results of MD trajectories on Ar_7 that demonstrate that melting loops found by earlier workers[3] were artifacts caused by insufficiently long runs. Similar findings have been reported for the Ar_{13} cluster.[23] Long trajectories are especially critical in the melting region of a small cluster since melting can be viewed as the onset of rapid isomerization of the cluster as new portions of phase space become accessible to the system. In the melting region, specific barrier effects can cause trapping of the system in a particular isomer for a disproportionate fraction of the total trajectory.

Several criteria indicate that Ar_7 melts in a fairly broad temperature range starting at about 16 K. The temperature at which melting occurs is consistent with the MC results of Etters and Kaelberer.[5,6] One indicator of the breadth of the transition is the length of the trajectory required to yield uniform uncertainty limits on T. The longest runs are required in the coexistence region.

In this paper we have emphasized the picture of the cluster as a nonrigid molecule which can undergo classical iso-

TABLE V. Rate tables obtained by dividing each entry in Table IV by the appropriate residence time t_i. See the text. Rates are in ns^{-1}.

$E=-14.499$	$T=14.98$			$E=-13.820$	$T=18.28$		
0.000	0.068	0.000	0.000	0.000	2.731	0.000	0.000
7.137	0.000	0.000	0.000	21.570	1.198	5.392	9.587
0.000	0.000	0.000	0.000	0.000	49.560	0.000	0.000
0.000	0.000	0.000	0.000	0.000	57.348	3.823	3.823
$E=-14.290$	$T=15.83$			$E=-13.561$	$T=19.37$		
0.000	0.285	0.000	0.000	0.000	5.083	0.086	0.775
5.575	0.000	2.230	1.115	29.110	0.939	14.555	20.189
0.000	107.049	0.000	0.000	2.712	92.222	0.000	2.712
0.000	160.574	0.000	0.000	7.147	51.222	4.765	2.382
$E=-14.216$	$T=16.39$			$E=-13.435$	$T=19.63$		
0.000	0.393	0.000	0.000	0.246	7.630	0.492	0.738
12.937	0.761	3.044	1.522	24.817	6.081	10.354	19.887
0.000	21.390	0.000	0.000	13.381	62.789	0.000	8.235
0.000	35.710	0.000	0.000	6.344	47.181	3.568	3.965
$E=-14.188$	$T=16.10$			$E=-13.318$	$T=20.39$		
0.000	0.694	0.000	0.000	0.094	8.471	0.471	1.412
5.853	0.669	3.177	2.508	37.398	4.774	17.108	29.043
1.305	23.490	0.000	0.000	12.496	68.728	0.000	3.124
0.000	12.870	0.000	0.000	6.848	65.051	5.136	3.424
$E=-14.039$	$T=17.17$			$E=-13.063$	$T=21.22$		
0.075	1.208	0.000	0.075	0.000	13.922	0.898	3.144
10.262	0.604	0.000	1.811	40.652	0.000	34.300	62.248
0.000	0.000	0.000	0.000	8.587	124.509	0.000	4.293
0.000	91.757	0.000	0.000	14.291	95.957	6.125	2.042
$E=-13.947$	$T=17.71$			$E=-11.630$	$T=27.79$		
0.000	1.424	0.150	0.000	0.000	69.144	11.524	30.505
17.488	0.000	3.180	4.770	114.398	25.545	104.402	198.809
0.000	35.421	0.000	0.000	45.083	257.237	15.912	18.563
0.000	34.907	0.000	0.000	44.717	178.867	11.179	55.896

merization reactions. This is because the quenching technique allows us to follow in great detail the system's passage through configuration space.

In their recent reexamination of the melting behavior of Ar_{13}, Jellinek, Beck, and Berry[23] have analyzed their trajectories in terms of the coexistence of solid and liquid forms of the cluster in the melting region. Solid Ar_{13} is essentially trapped in the lowest isomer of the cluster, an icosahedron. The liquid form visits isomers of higher energy than the icosahedron. Since Ar_{13} has many more isomers than Ar_7 (recall that the number of isomers increases roughly exponentially with N), the quenching technique with complete characterization of isomer geometry and permutational identity will be much harder to apply to Ar_{13}.

We note that the Ar_7 coexistence region appears to be broader than that for Ar_{13} as expected from general scaling considerations.[30,31] In microscopic terms, the large number of high energy isomers occurring at nearly the same energy leads to a sharper transition in Ar_{13} than in Ar_7. This is borne out by simulations of a wide range of cluster sizes.[32] A number of problems remain to be pursued in Ar_7. As mentioned above, the locations of the lowest energy saddles between isomers are currently being obtained and the characterization of the isomerization coordinates is in progress. An interesting use of these quantities is to study the nonlinear dynamics of a system with many degrees of freedom. How should isomerization rates be computed, taking rapid recrossing into account? The Ar_7 system may also be a valuable numerical testing ground for characterizing the ergodic properties of high dimensional systems. Farantos, for example, has investigated the stochastic nature of Ar_4 trajectories as a function of energy.[33] The Ar_7 case should be far richer with perhaps only a modest increase in computational effort.

The importance of tetrahedral, icosahedral and other "magic" number packing geometries in the interpretation of structure factors of larger amorphous solid clusters of argon has been demonstrated.[19] These highly ordered local structures are also important in glassy materials. Detailed investigation of the collective coordinates responsible for melting of small clusters—especially the extra stable Ar_4, Ar_7, and Ar_{13} will be of great interest in understanding how these highly ordered local structures form in glassy materials.

ACKNOWLEDGMENTS

F. A. would like to thank Research Corporation and the Computer Applications Network at the University of Maine for support and computer time respectively. F. A. also thanks Professor Bruce Berne for helpful discussions and support under a grant from the National Science Foundation during the preliminary stages of this work. R. S. B. acknowledges support from a National Science Foundation Grant. Finally, we acknowledge the opportunity afforded by the Telluride Summer Research Center to work on a portion of this manuscript.

[1]D. J. McGinty, J. Chem. Phys. **58**, 4733 (1973).
[2]W. D. Kristensen, E. J. Jensen, and R. M. J. Cotterill, J. Chem. Phys. **60**, 11 (1974).
[3]C. L. Briant and J. J. Burton, J. Chem. Phys. **63**, 2045 (1975).
[4]R. D. Etters and J. Kaelberer, Phys. Rev. A **11**, 1068 (1975).
[5]J. B. Kaelberer and R. D. Etters, J. Chem. Phys. **66**, 3233 (1977).
[6]R. D. Etters and J. B. Kaelberer, J. Chem. Phys. **66**, 5112 (1977).
[7]R. D. Etters, R. Danilowicz, and J. Kaelberer, J. Chem. Phys. **67**, 4145 (1977).
[8]F. F. Abraham, *Homogeneous Nucleation Theory* (Academic, New York, 1974).
[9]N. Quirke and P. Sheng, Chem. Phys. Lett. **110**, 63 (1984).
[10]G. Natanson, F. G. Amar, and R. S. Berry, J. Chem. Phys. **78**, 399 (1983).
[11]G. S. Ezra, Mol. Phys. **38**, 863 (1979).
[12]G. Natanson, in *Advances in Chemical Physics*, edited by I. Prigogine and S. A. Rice (Wiley–Interscience, New York, 1985), Vol. 58, p. 55.
[13]P. R. Bunker, *Molecular Symmetry and Spectroscopy* (Academic, New York, 1979).
[14]F. H. Stillinger and T. A. Weber, Phys. Rev. A **25**, 978 (1982).
[15]F. H. Stillinger and T. A. Weber, J. Phys. Chem. **87**, 2833 (1983).
[16]R. A. LaViolette and F. H. Stillinger, J. Chem. Phys. **83**, 4079 (1985); F. H. Stillinger and T. A. Weber, Phys. Rev. A **28**, 2408 (1983).
[17]K. Huang, *Statistical Mechanics* (Wiley, New York, 1963).
[18]M. R. Hoare and P. Pal, J. Cryst. Growth **17**, 77 (1972).
[19]J. Farges, M. F. de Feraudy, B. Raoult, and G. Torchet, J. Chem. Phys. **78**, 5067 (1983), and references contained therein.
[20]L. S. Bartell, R. K. Heenan, and M. Nagashima, J. Chem. Phys. **78**, 236 (1983).
[21]S. S. Kim and G. D. Stein, Rev. Sci. Instrum. **53**, 838 (1982); D. Abraham, J. H. Binn, B. G. DeBoer, and G. D. Stein, Phys. Fluids **24**, 1017 (1981); O. Abraham, S. S. Kim, and G. D. Stein, J. Chem. Phys. **75**, 402 (1981).
[22]I. A. Harris, R. S. Kidwell, and J. A. Northby, Phys. Rev. Lett. **53**, 2390 (1984).
[23]J. Jellinek, T. L. Beck, and R. S. Berry, J. Chem. Phys. **84**, 2783 (1986).
[24]J. Kushick and B. Berne, in *Statistical Mechanics. Part B. Time Dependent Processes*, edited by B. Berne (Plenum, New York, 1977), Vol. 6, Chap. 2.
[25]R. S. Berry, J. Chem. Phys. **32**, 447 (1960).
[26]R. S. Berry, J. Jellinek, and G. Natanson, Chem. Phys. Lett. **107**, 227 (1984); Phys. Rev. A **30**, 914 (1984).
[27]S. K. Schiferl and D. C. Wallace, J. Chem. Phys. **83**, 5203 (1985).
[28]W. Forst, *Theory of Unimolecular Reactions* (Academic, New York, 1973).
[29]B. J. Berne, N. DeLeon, and R. O. Rosenberg, J. Phys. Chem. **86**, 2166 (1982).
[30]M. E. Fisher and A. N. Berker, Phys. Rev. B **26**, 2507 (1982).
[31]Y. Imry, Phys. Rev. B **21**, 2042 (1980).
[32]T. Beck, J. Jellinek, and R. S. Berry (to be published).
[33]S. C. Farantos, J. Phys. Chem. **87**, 5061 (1983).